Inorg. Chem. **2007**, *46*, 8008–8018

Inorganic Chemistry
Article

Analysis of Uranium Azide and Nitride Complexes by Atmospheric Pressure Chemical Ionization Mass Spectrometry

William J. Evans,* Kevin A. Miller, Joseph W. Ziller, and John Greaves

Department of Chemistry, University of California, Irvine, California 92697-2025

Received March 30, 2007

Atmospheric pressure chemical ionization mass spectrometry (APCI-MS) has been used to characterize the air-sensitive paramagnetic organouranium azide and nitride complexes $[(C_5Me_5)_2UN_3(\mu\text{-}N_3)]_3$ and $[(C_5Me_5)U(\mu\text{-}I)_2]_3N$, respectively. The trimetallic complex $[(C_5Me_5)U(\mu\text{-}I)_2]_3E$ had been identified by X-ray crystallography, but the data did not definitively identify E as N^{3-} versus O^{2-} or $(OH)^-$, a common problem in heavy-element nitride complexes involving metals with variable oxidation states. A comparison of the 250 °C APCI-MS spectra of products made from NaN_3 and $Na^{15}NNN$ showed mixed $[M]^+$ and $[M + H]^+$ envelopes at expected ion intensities for the ^{14}N and ^{15}N isotopomers. A compilation of U–C(C_5Me_5) and U–I bond distance data for U^{3+} and U^{4+} is also reported that shows that the ranges for the two oxidation states have significant overlap.

Introduction

Recent results in uranium azide chemistry have indicated that this metal−ligand combination is likely to be quite useful in the production of new structures and reactivity patterns. For example, the first actinide polyazide complex, the heptaazide $(Bu_4N)_3U(N_3)_7$,[1] has been isolated (eq 1), and the mixed azide nitride $[(C_5Me_5)_2U(\mu\text{-}N)(C_5Me_5)_2U(\mu\text{-}N_3)]_4$[2] has been isolated from the reaction of $[(C_5Me_5)_2U][BPh_4]$ and NaN_3 (eq 2). The latter complex is unusual in both its large 24-atom uranium−nitrogen ring structure and the nearly linear UNU linkages. Complexes of this type that are dense in uranium and nitrogen may be of interest as molecular precursors to high-purity UN, a potential nuclear fuel of the future.[3,4]

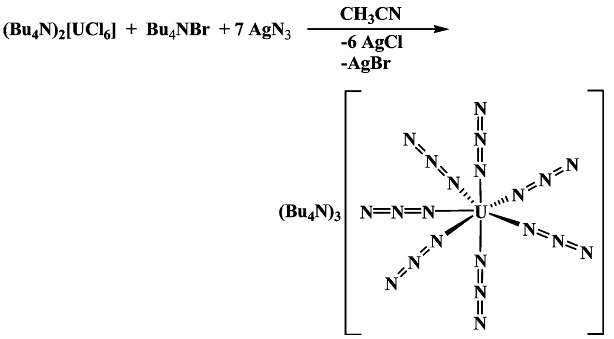

(1)

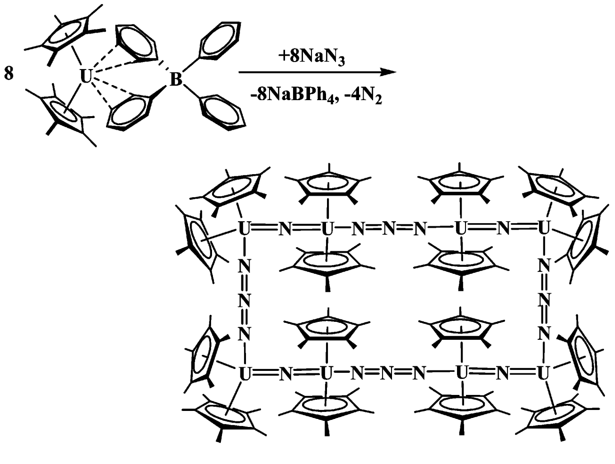

(2)

To expand the range of uranium complexes of this type, the reactions of some well-known organouranium halides with sodium azide were examined. In the case of the tetravalent precursor, $(C_5Me_5)_2UCl_2$,[5] an azide derivative, $[(C_5Me_5)_2UN_3(\mu\text{-}N_3)]_3$ (**1**), was isolated and completely identified by X-ray crystallography.

---

* To whom correspondence should be addressed. E-mail: wevans@uci.edu.

(1) Crawford, M.-J.; Ellern, A.; Mayer, P. *Angew. Chem., Int. Ed.* **2005**, *44*, 7874.

(2) Evans, W. J.; Kozimor, S. A.; Ziller, J. W. *Science* **2005**, *309*, 1835.

(3) Black, L.; et al. *J. Alloys Compds.* **2001**, *315*, 36.

(4) Reshetnikov, F. G. *At. Energ.* **2001**, *91*, 998.

(5) Marks, T. J.; Fagan, P. J.; Manriquez, J. M.; Maatta, E. A.; Seyam, A. M. *J. Am. Chem. Soc.* **1981**, *103*, 6650.

10.1021/ic7006099 CCC: $37.00

With the trivalent starting material, $(C_5Me_5)UI_2(THF)_3$,[6] no azide was isolated, but instead a trimetallic complex, $[(C_5Me_5)U(\mu\text{-}I)_2]_3E$ (**2**), was obtained that appeared to contain a nitride ion. Although the X-ray crystallographic data were consistent with an N^{3-} ion in this complex, this method of analysis was not able to differentiate the nitride from oxide or hydroxide. Because the three uranium atoms in the structure could have variable oxidation states, any of these options were possible. Differentiating nitrogen from oxygen in the presence of large metals of variable oxidation state is a general problem in heavy-metal chemistry.[7,8] Because the electropositive f elements are so oxophilic, it is always possible to incorporate oxide or hydroxide inadvertently into structures.[9−17]

We report here the use of atmospheric pressure chemical ionization mass spectrometry (APCI-MS) to resolve the nitride problem and to test its general application to complexes of this type. We also present a compilation of $U-C(C_5Me_5)$ and U−I bond distance data for U^{3+} and U^{4+} metallocenes that was assembled to determine if this would be useful in identifying E in **2**. With organolanthanide complexes, it is often possible to differentiate oxidation states on the basis of $M-C(C_5Me_5)$ bond lengths.[18,19]

Experimental Section

The manipulations described below were performed under nitrogen with the rigorous exclusion of air and water using Schlenk, vacuum-line, and glovebox techniques. Solvents were dried over Q-5 and molecular sieves. NMR solvents were dried over a sodium−potassium alloy and vacuum-transferred before use. NMR spectra were recorded with a Bruker DRX 500 MHz system. IR spectra were recorded as thin films on an ASI ReactIR 1000 instument.[20] $(C_5Me_5)_2UCl_2$[5] and $(C_5Me_5)UI_2(THF)_3$[6] were prepared as previously described. NaN_3 and $Na^{15}NNN$ were purchased from Aldrich and placed under vacuum (10^{-3} Torr) 12 h before use. Elemental analyses were performed by Analytische Laboratorien, Lindlar, Germany. APCI-MS spectra were collected on a Waters (Micromass) LCT Premier orthogonal time-of-flight mass spectrometer. Toluene was used as the analyte solvent and to generate the reagent ions. The corona discharge was set very low at 1 μA, and the temperature of the APCI-MS probe was critical for obtaining molecular weight information. Because of the air and water sensitivity of the samples, syringes were loaded with the analyte dissolved in toluene while in the glovebox. The syringe needles were sealed with a septum and brought to the mass spectrometer for immediate analysis.

$[(C_5Me_5)_2UN_3(\mu\text{-}N_3)]_3$ (1). In a nitrogen-filled glovebox, $(C_5Me_5)_2UCl_2$ (264 mg, 0.456 mmol) in tetrahydrofuran (THF; 5 mL) was added to a stirred slurry of NaN_3 (59 mg, 0.91 mmol) in THF (2 mL). After the solution was stirred for 12 h, the solution was centrifuged to remove a red−brown precipitate. The precipitate was washed three times with THF and discarded. The THF washings were combined with the dark-red supernatant and evaporated to dryness to yield **1** as a dark-red crystalline powder (248 mg, 92%). Crystals of **1** suitable for X-ray diffraction were grown at 25 °C from a concentrated THF/toluene solution. ^1H NMR (500 MHz, C_6D_6): δ 0.67 (s, 30H, C_5Me_5, $\Delta\nu_{1/2} = 20$ Hz). ^{13}C NMR (500 MHz, C_6D_6): δ −41.4 (C_5*Me*$_5$), 126.0 (*C*$_5Me_5$). IR: 2964s, 2918s, 2856s, 2111vs, 2073vs, 1586w, 1490w, 1447m, 1351m, 1316w, 1258vs, 1065vs, 1011vs, 865s, 803s, 702s cm^{-1}. Anal. Calcd for $C_{60}H_{90}N_{18}U_3$: C, 40.54; H, 5.10; N, 14.18; U, 40.17. Found: C, 40.41; H, 5.12; N, 14.29; U, 40.58.

$[(C_5Me_5)U(\mu\text{-}I)_2]_3N$ (2). In a nitrogen-filled glovebox, a blue-green solution of $(C_5Me_5)UI_2(THF)_3$ (254 mg, 0.301 mmol) in THF (10 mL) was added to a stirred slurry of NaN_3 (10 mg, 0.151 mmol) in THF (2 mL). The solution became dark-red after 20 min. After the mixture was stirred overnight, the dark-red solution was evaporated to a tacky oil that was dissolved in toluene and allowed to stir for 2 h. The dark-red solution was centrifuged, and a white insoluble material was removed. Evaporation of the supernatant yielded a dark red oil that was dissolved in a 1:1 hexane/toluene solution and cooled to −35 °C. After 1 day, **2** was obtained as dark-red crystals (62 mg, 33%). Crystals of **2** suitable for X-ray diffraction were grown at −35 °C from a concentrated hexane solution. ^1H NMR (C_6D_6): δ 25.5 (br s, C_5Me_5, $\Delta\nu_{1/2} = 135$ Hz). IR: 2971m, 2943m, 2903s, 2857m, 2099w, 1483w, 1450m, 1431m, 1378s, 1262w, 1023w, 802w, 601vs cm^{-1}. Anal. Calcd for $C_{30}H_{45}I_6NU_3$: C, 19.01; H, 2.39; N, 0.75; U, 37.68; I, 40.18. Found: C, 17.71; H, 2.44; N, 1.02; U, 38.40; I, 39.90.

X-ray Data Collection, Structure Solution, and Refinement of 1. A red crystal of approximate dimensions 0.07 × 0.14 × 0.21 mm was mounted on a glass fiber and transferred to a Bruker CCD platform diffractometer. The *SMART*[21] program package was used to determine the unit-cell parameters and for data collection (25 s $frame^{-1}$ scan time for a sphere of diffraction data). The raw frame data were processed using *SAINT*[22] and *SADABS*[23] to yield the reflection data file. Subsequent calculations were carried out using the *SHELXTL*[24] program. The diffraction symmetry was *mmm*, and the systematic absences were consistent with the orthorhombic space groups $Pna2_1$ and *Pnma*. It was later determined that the centrosymmetric space group *Pnma* was correct. The structure was solved by direct methods and refined on F^2 by full-matrix least-

---

(6) Avens, R. L.; Burns, C. J.; Butcher, R. J.; Clark, D. L.; Gordon, J. C.; Schake, A. R.; Scott, B. L.; Watkin, J. G.; Zwick, B. D. *Organometallics* **2000**, *19*, 451.

(7) Korobkov, I.; Gambarotta, S.; Yap, G. P. A. *Angew. Chem., Int. Ed.* **2002**, *41*, 3433.

(8) Korobkov, I.; Gambarotta, S.; Yap, G. P. A. *Organometallics* **2001**, *20*, 2552.

(9) Evans, W. J.; Kozimor, S. A.; Ziller, J. W. *Polyhedron* **2004**, *23*, 2689.

(10) Evans, W. J.; Davis, B. L.; Nyce, G. W.; Fujimoto, C. H.; Ziller, J. W. *J. Organomet. Chem.* **2003**, *677*, 89.

(11) Evans, W. J.; Allen, N. T.; Greci, M. A.; Ziller, J. W. *Organometallics* **2001**, *20*, 2936.

(12) Evans, W. J.; Hozbor, M. A.; Bott, S. G.; Robinson, G. H.; Atwood, J. L. *Inorg. Chem.* **1988**, *27*, 1990.

(13) Schumann, H.; Keitsch, M. R.; Demtschuk, J.; Molander, G. A. *J. Organomet. Chem.* **1999**, *582*, 70.

(14) Deng, D.; Song, F.; Wang, Z.; Qian, C.; Wu, G.; Zheng, P. *Polyhedron* **1992**, *11*, 2883.

(15) Hitchcock, P. B.; Lappert, M. F.; Prasher, S. *J. Organomet. Chem.* **1991**, *413*, 79.

(16) Xie, Z.; Liu, Z.; Chui, K.; Xue, F.; Mak, T. C. W. *J. Organomet. Chem.* **1999**, *588*, 78.

(17) Hermann, W. A.; Anwander, R.; Kleine, M.; Ofele, F.; Riede, J.; Scherer, W. *Chem. Ber.* **1992**, *125*, 2391.

(18) Evans, W. J.; Foster, S. E. *J. Organomet. Chem.* **1992**, *433*, 79.

(19) Shannon, R. D. *Acta Crystallogr.* **1976**, *A23*, 751.

(20) Evans, W. J.; Johnston, M. A.; Ziller, J. W. *Inorg. Chem.* **2000**, *39*, 3421.

(21) *SMART Software Users Guide*, version 5.1; Bruker Analytical X-Ray Systems, Inc.: Madison, WI, 1999.

(22) *SAINT Software Users Guide*, version 6.0; Bruker Analytical X-Ray Systems, Inc.: Madison, WI, 1999.

(23) Sheldrick, G. M. *SADABS*, version 2.10; Bruker Analytical X-Ray Systems, Inc.: Madison, WI, 2002.

(24) Sheldrick, G. M. *SHELXTL*, version 6.12; Bruker Analytical X-Ray Systems, Inc.: Madison, WI, 2001.

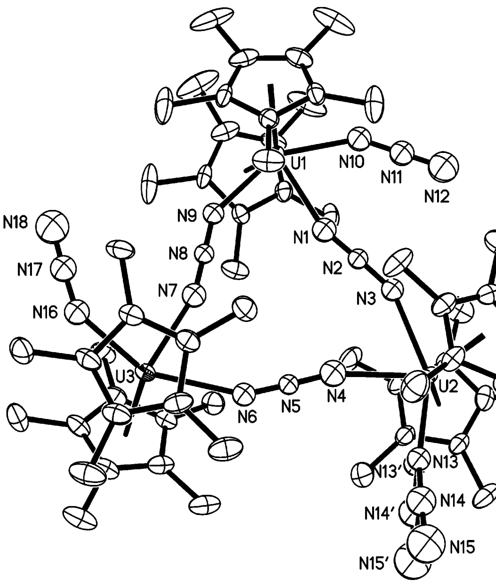

Figure 1. Molecular structure of **1** with thermal ellipsoids drawn at the 30% probability level.

Table 1. X-ray Data Collection Parameters for **1** and **2**

empirical formula	$C_{60}H_{90}U_3N_{18}{\cdot}C_4H_8O{\cdot}C_7H_8$ (**1**$\cdot C_4H_8O{\cdot}C_7H_8$)	$C_{30}H_{45}I_6NU_3{\cdot}C_6H_{14}$ (**2**$\cdot C_6H_{14}$)
fw	1941.83	1981.33
temp (K)	168(2)	163(2)
cryst syst	orthorhombic	monoclinic
Space group	*Pnma*	$P2_1/n$
a (Å)	30.049(3)	12.3088(12)
b (Å)	15.5193(15)	25.188(2)
c (Å)	15.8201(15)	16.3565(16)
α (deg)	90	90
β (deg)	90	109.486(2)
γ (deg)	90	90
V (Å^3)	7465.8(13)	4780.6(8)
Z	4	4
ρ_{calcd} (Mg m^{-3})	1.728	2.753
μ (mm^{-1})	6.545	14.036
R1 [$I > 2.0\sigma(I)$]^a	0.0418	0.0215
wR2 (all data)^a	0.1053	0.0456

[a] Definitions: $\mathrm{wR2} = [\sum[w(F_o^2 - F_c^2)^2]/\sum[w(F_o^2)^2]]^{1/2}$; $\mathrm{R1} = \sum||F_o| - |F_c||/\sum|F_o|$.

squares techniques. The analytical scattering factors[25] for neutral atoms were used throughout the analysis. Hydrogen atoms were included using a riding model. The molecule was located on a mirror plane. Nitrogen atoms N13, N14, and N15 were displaced from the mirror plane and included using partial site-occupancy factors. There was one molecule of THF and one molecule of the toluene solvent present. Each was located on a mirror plane. The toluene molecule was disordered and included as above for the disordered nitrogen atoms. Least-squares refinement yielded wR2 = 0.1053 and GOF = 1.063 for 395 variables refined against 6619 data (0.85 Å). As a comparison for refinement on F, R1 = 0.0418 for those 4892 data with $I > 2.0\sigma(I)$. It was necessary to refine the nitrogen atoms, the coordinated THF molecule, and the solvent molecules isotropically. Anisotropic refinement resulted in several atoms becoming non-positive-definite. Details are given in Table 1.

X-ray Data Collection, Structure Solution, and Refinement of 2. A dark-red crystal of approximate dimensions 0.11 × 0.21 × 0.28 mm was handled as described for **1**. The diffraction symmetry was $2/m$, and the systematic absences were consistent with the centrosymmetric monoclinic space group $P2_1/n$, which was later determined to be correct. The structure was solved by direct methods and refined on F^2 by full-matrix least-squares techniques. The analytical scattering factors[25] for neutral atoms were used throughout the analysis. Hydrogen atoms were included using a riding model. There was one molecule of the hexane solvent present per formula unit. At convergence, wR2 = 0.0456 and GOF = 1.127 for 430 variables refined against 11 815 data. As a comparison for refinement on F, R1 = 0.0215 for those 10 448 data with $I > 2.0\sigma(I)$. Details are given in Table 1.

Results and Discussion

Compound 1. $(C_5Me_5)_2UCl_2$ reacts readily with NaN_3 to make a dark red complex with a single resonance in the ^{1}H NMR spectrum. The complex was identified by X-ray crystallography as the trimetallic azide **1** (Figure 1). It was isolated in >90% yield (eq 3).

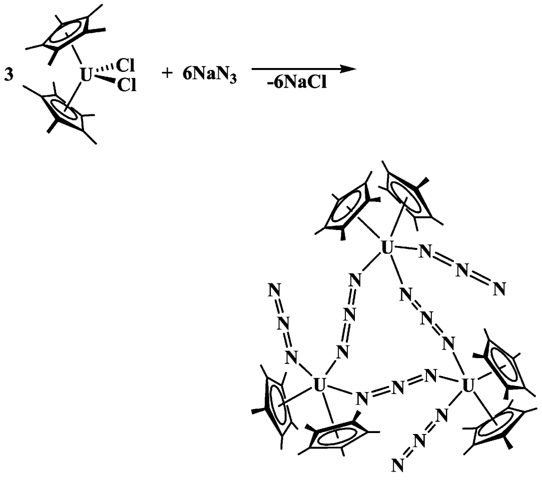

1

(3)

Each uranium in **1** is attached to two bridging azide ligands and one terminal azide. Although the diffraction experiment revealed the structure, the quality of the data was not sufficient for detailed structural analysis. Within the error limits, the metrical parameters involving uranium and the azides are similar to those in $(Bu_4N)_3[U(N_3)_7]$[1] and $[(C_5Me_5)_2U(\mu\text{-}N)(C_5Me_5)_2U(\mu\text{-}N_3)]_4$.[2]

Compound 2. In contrast to eq 3, the reaction of NaN_3 with trivalent $(C_5Me_5)UI_2(THF)_3$ did not generate the ionic metathesis product in which the halides were replaced by azide. The product isolated and identified by X-ray crystallography (Figure 2) was **2**, a complex that still incorporated all of the anionic ligands attached to uranium in the starting material.

In the center of the trimetallic complex was an atom that could be a nitride ligand made by reduction of azide by the U^{3+} starting material according to eq 4 and the half-reaction in Scheme 1. If each of the uranium atoms in **2** were

Scheme 1

$$6U^{3+} \rightarrow 6U^{4+} + 6e^-$$

$$3N_3^- + 6e^- \rightarrow 3N_2 + 3N^{3-}$$

---

(25) *International Tables for X-Ray Crystallography*; Kluwer Academic Publishers: Dordrecht, The Netherlands, 1992; Vol. C.

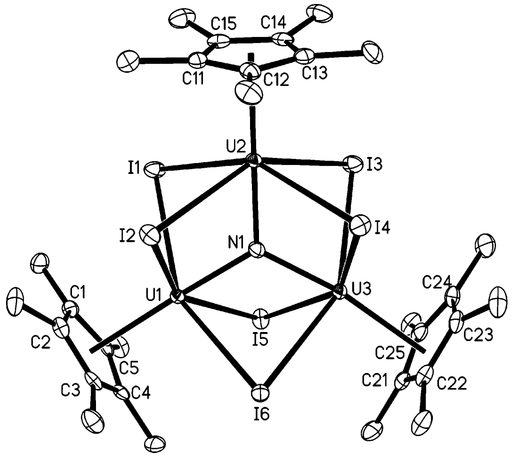

Figure 2. Molecular structure of **2** with thermal ellipsoids drawn at the 50% probability level.

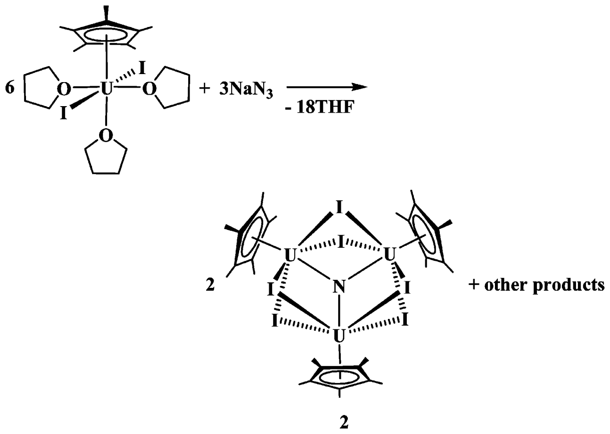

(4)

tetravalent, the overall charge would be balanced with the central atom as N^{3-}. However, if the central atom were O^{2-} and one of the uranium atoms were U^{3+}, there still would be charge balance. Likewise, a central $(OH)^-$ group with two U^{3+} centers would be charge balanced. The bond distances to each uranium in **2** were sufficiently similar (Table 2) that the complex did not appear to contain different types of uranium centers. However, if there were disorder in the position of the metal of a different oxidation state, differences might not be observable.[26] ^{15}N NMR spectroscopy was conducted with a sample of **2** made from $Na^{15}NNN$ to determine the identity of the central atom. However, no resonances were observed over a sweep width of 500 ppm from −250 to +250 ppm. However, it can be difficult to identify ^{15}N NMR resonances in paramagnetic f element complexes.[27]

U^{3+} versus U^{4+} Bond Distance Analogues. It was of interest to see if U−C(C_5Me_5), U−(C_5Me_5 ring centroid), and U−I distances would be useful to differentiate trivalent and tetravalent uranium complexes and aid in the identification of **2**. This would provide another metric to evaluate cases in which the oxidation state is uncertain. In the lanthanide series, Ln^{2+} bond distances are generally 0.1 Å longer than those for analogous Ln^{3+} complexes. For example, eight-coordinate complexes containing the trivalent $[(C_5Me_5)_2Sm]^+$ unit have a 2.68(1)−2.80(1) Å range of Sm−C(C_5Me_5) distances, whereas eight coordinate complexes containing divalent $(C_5Me_5)_2Sm$ have a 2.82(3)−2.86(3) Å range. Although there is overlap between these ranges within the error limits, the trend for longer distances for the lower valent metal is clear.

Table 2. Selected Bond Distances (Å) and Angles (deg) for **2**

U1−Cnt1	2.455	U1−C(C_5Me_5) range	2.719(4)−2.757(4)
U2−Cnt2	2.462	U2−C(C_5Me_5) range	2.717(4)−2.764(4)
U3−Cnt3	2.457	U3−C(C_5Me_5) range	2.708(4)−2.761(4)
U1−N1	2.152(3)	U1−C(C_5Me_5) avg	2.73(2)
U2−N1	2.138(3)	U2−C(C_5Me_5) avg	2.74(2)
U3−N1	2.157(3)	U3−C(C_5Me_5) avg	2.73(2)
U1−I1	3.1536(4)	U−C(C_5Me_5) avg	2.74(2)
U1−I6	3.1599(4)	U−Cnt avg	2.458
U1−I2	3.1623(4)	Cnt1−U1−N1	178.1
U1−I5	3.1720(4)	Cnt2−U2−N1	178.6
U2−I1	3.1586(4)	Cnt3−U3−N1	178.1
U2−I4	3.1617(4)	Cnt1−U1−I range	103.4−106.7
U2−I3	3.1632(4)	Cnt2−U2−I range	103.9−106.1
U2−I2	3.2109(4)	Cnt3−U3−I range	103.4−107.4
U3−I4	3.1483(4)	U2−U3−U1	59.985(8)
U3−I6	3.1622(4)	U2−U1−U3	59.710(4)
U3−I3	3.1648(4)	U3−U2−U1	60.305(6)
U3−I5	3.1825(4)		

To determine if similar trends exist in organoactinide structures, metrical data on 43 examples of trivalent and tetravalent uranium $(C_5Me_5)^-$ complexes in the Cambridge Crystallographic Data Centre database were examined and compiled (Table 3). Because the Shannon radius[19] for six-coordinate U^{3+} is 1.025 Å versus 0.89 Å for U^{4+}, a differentiation seemed possible. Metallocenes are analyzed here in detail because they constitute the bulk of examples in the table.

This survey shows that although trivalent metallocenes on average have longer U−C(C_5Me_5) and U−(C_5Me_5 ring centroid) distances, which is consistent with the Shannon radii, there is significant overlap in the ranges of values for U^{3+} and U^{4+} complexes. The average U−(C_5Me_5 ring centroid) distance of the 6 eight-coordinate U^{3+} structures is 2.51 Å compared to 2.42 Å for 16 eight-coordinate U^{4+} structures. However, the range of U−(C_5Me_5 ring centroid) distances of the 6 eight-coordinate U^{3+} complexes in Table 3 is 2.46−2.55 Å compared to a range of 2.42−2.53 Å for the 16 eight-coordinate U^{4+} complexes.

Hence, on average, the U^{3+} distances are longer, but the ranges overlap so much that it is difficult to use this criterion for any specific complex. In the case of complex **2**, the 2.444, 2.455, and 2.455 Å U−(C_5Me_5) ring centroid distances are formally in the range of the distances for U^{4+} metallocenes, but they are also close to the range for U^{3+}. The distances in the trivalent monoring precursor $(C_5Me_5)UI_2(THF)_3$ are 2.504 and 2.521 Å. No conclusion on oxidation state can be drawn from these data.

The 2.48−2.63 Å spread of distances found for 12 nine-coordinate U^{4+} structures (2.50 Å average) also overlaps the other ranges. Because hydride ligands are difficult to locate crystallographically in the presence of uranium, an $(n + 1)$-

---

(26) Parkin, G. *Acc. Chem. Res.* **1992**, *25*, 455.
(27) Evans, W. J.; Rego, D. B.; Ziller, J. W. *Inorg. Chem.* **2006**, *45*, 10790.

Table 3. Bond Distances (Å) and Angles (deg) of Trivalent and Tetravalent Uranium Metallocenes from the Cambridge Crystallographic Data Centre Database Arranged in Order of Increasing U−C(C_5Me_5) Average within Each Oxidation State/ Coordination Number Category

complex	oxid. state	coord. no.	U−C(C_5Me_5) range	U−C(C_5Me_5) avg	U−Cnt[a]	Cnt−U−Cnt[a]
$[(C_5Me_5)_2U]_2(\mu\text{-O})$[30]	3	7	2.676(9)−2.823(9)	2.74(3)	2.455 2.459 2.465 2.487 2.467[b]	134.5 132.6 133.6[b]
$\{[(Me_3Si)_2N](C_5Me_5)U\}_2(\mu\text{-}\eta^6{:}\ \eta^6\text{-}C_6H_6)$[31]	3	7	2.766(3)−2.795(3)	2.78(1)	2.506	
$(C_5Me_5)_2U[N(SiMe_3)_2]$[32]	3	7	2.791(3)−2.826(3)	2.80(1)	2.523 2.532 2.528[b]	132.4
	---------	---------				
$[(C_5Me_5)_2U(THF)_2][BPh_4]$[33]	3	8	2.68(2)−2.75(1)	2.72(2)	2.46	134.2
$[(C_5Me_5)_2U(\mu\text{-Cl})]_3$[34]	3	8		2.76(3)	2.48[b]	127.9
$(C_5Me_5)UI_2(THF)_3$[6]	3	8		2.77(1) 2.80(1)	2.521 2.504	
$[Na(18\text{-crown-6})(THF)_2][(C_5Me_5)_2U(dddt)]$[c,35]	3	8	2.766(7)−2.835(6)	2.79(2)	2.506 2.529 2.518[b]	135.7
$(C_5Me_5)_2UI(C_3Me_4N_2)$[36]	3	8	2.765(5)−2.841(5)	2.80(2)	2.514 2.532 2.523[b]	135.2
$[Na(18\text{-crown-6})(THF)_2][(C_5Me_5)_2U(S^iPr)_2]$[37]	3	8	2.786(3)−2.823(3)	2.81(1)	2.525 2.548 2.537[b]	133.8
	---------	---------				
$[(C_5Me_5)_2U]_2(\mu\text{-}\eta^6{:}\ \eta^6\text{-}C_6H_6)$[31]	3	9	2.795(14)−2.878(14)	2.83(3)	2.564 2.567 2.566 2.583 2.570[b]	121.1 121.7 121.4[b]
	---------	---------				
$[(C_5Me_5)_2U][BPh_4]$[32]	3	10	2.753(7)−2.830(8)	2.78(3)	2.490 2.516 2.503[b]	132.7
	---------	---------				
$(C_5Me_5)_2U(N\text{-}2,4,6\text{-}t\text{-}Bu_3C_6H_2)$[38]	4	7		2.790(12)	2.515	133.8
	---------	---------				
$[(C_5Me_5)_2UMe(THF)][MeBPh_3]$[39]	4	8	2.67(1)−2.75(1)	2.71(2)	2.428 2.435 2.432[b]	140.0
$(C_5Me_5)_3U_3(\mu_3\text{-I})(\mu_3\text{-S})(\mu_2\text{-I})_3I_3$[40]	4	8	2.62(7)−2.78(7)	2.71(6)	2.422 2.420 2.467 2.436[b]	
$(C_5Me_5)_2UMe_2$[41]	4	8	2.694(4)−2.774(4)	2.73(2)	2.456 2.462 2.459[b]	140.4
$(C_5Me_5)_2U(dddt)$[c,35]	4	8	2.676(13)−2.753(13)	2.73(2)	2.451 2.458 2.455[b]	133.1
$(C_5Me_5)_2U(SMe)_2$[42]	4	8	2.71(1)−2.77(1)	2.73(2)	2.47(2)	137.6
$(C_5Me_5)_2U(BH_4)_2$[43]	4	8	2.71(6)−2.77(9)	2.74(2)	2.46(4) 2.48(4) 2.47(1)[b]	133.1
$[(C_5Me_5)_2U(OCH_3)]_2PH$[44]	4	8	2.70(2)−2.80(2)	2.74(3)	2.462 2.483 2.452[b]	133.1
$(C_5Me_5)_2U(C_4Ph_4)$[45]	4	8	2.731(3)−2.774(3)	2.75(2)	2.476	142.6
$[Li(tmed)][(C_5Me_5)_2U(NC_6H_5)Cl]$[d,38]	4	8		2.77(2)	2.492 2.494 2.493[b]	132.4
$(C_5Me_5)_2U(N{=}CPh_2)_2$[46]	4	8	2.724(7)−2.811(6)	2.77(3)	2.483 2.506 2.495[b]	141.0
$(C_5Me_5)_2U[N{=}C(CH_2C_6H_5)(tpy)]_2$[e,47]	4	8	2.757(6)−2.779(7)	2.77(8)	2.486	136.8
$[(C_5Me_5)_2U\{NH(C_6H_3Me_2\text{-}2,6)\}_2]$[48]	4	8	2.731(5)−2.802(7)	2.78(3)	2.562	127.8

Table 3. Cont'd.

complex	oxid. state	coord. no.	U−C(C_5Me_5) range	U−C(C_5Me_5) avg	U−Cnt[a]	Cnt−U−Cnt[a]
$[(C_5Me_5)_2U(\mu\text{-}N)U(\mu\text{-}N_3)(C_5Me_5)_2]_4$[2]	4	8	2.700(9)−2.876(11)	2.78(4)	2.490 2.499 2.507 2.508 2.514 2.521 2.521 2.527 2.511[b]	128.2 128.4 128.3 126.2 127.8[b]
$(C_5Me_5)_2U(P\text{-}2,4,6\text{-}t\text{-}Bu_3C_6H_2)(OPMe_3)$[49]	4	8	2.753(6)−2.835(5)	2.79(2)	2.513 2.518 2.516[b]	131.4
$[Na(18\text{-}crown\text{-}6)(THF)_2][(C_5Me_5)_2U(S^tBu)(S)]$[50]	4	8	2.754(6)−2.841(7)	2.79(3)	2.502 2.520 2.511[b]	130.7
$(C_5Me_5)_2U(O)[C(NMeCMe)_2]$[30]	4	8	2.715(9)−2.871(9)	2.80(5)	2.523 2.527 2.525[b]	136.3
	---------	---------				
$(C_5Me_5)_2UI_2(NCPh)$[51]	4	9	2.62(2)−2.81(2)	2.74(5)	2.45(2) 2.48(2) 2.47(2)[b]	136.7
$(C_5Me_5)_2U(S^tBu)(S_2C^tBu)$[42]	4	9	2.71(2)−2.80(2)	2.75(3)	2.47(2) 2.49(2) 2.48(1)[b]	133.3
$(C_5Me_5)_2UCl(\eta^2\text{-}{}^tBuNSPh)$[52]	4	9	2.72(2)−2.80(2)	2.76(2)	2.487 2.501 2.494[b]	128.42
$(C_5Me_5)_2U(CH_2C_6H_5)[\eta^2\text{-}(O,C)\text{-}ONC_5H_4]$[53]	4	9	2.732(14)−2.795(13)	2.77(2)	2.481 2.501 2.491[b]	135.3
$[(C_5Me_5)_2U(NMe_2)(CN^tBu)_2][BPh_4]$[54]	4	9	2.74(1)−2.80(1)	2.77(2)	2.49 2.50 2.50[b]	130.9
$(C_5Me_5)_2UCl_2(HNPPh_3)$[55]	4	9	2.74(1)−2.81(1)	2.77(2)	2.49(4) 2.50(4) 2.495(5)[b]	134
$(C_5Me_5)_2UCl_2(HNSPh_2)$[56]	4	9	2.69(2)−2.89(2)	2.77(6)	2.48 2.52 2.50[b]	130.7
$(C_5Me_5)_2UCl(OH)(HNSPh_2)_2$[57]	4	9	2.73(1)−2.81(2)	2.78(2)	2.497 2.499 2.501 2.511 2.502[b]	135.8
$(C_5Me_5)_2UCl[(CH_2)(CH_2)P(Ph)(Me)]$[58]	4	9	2.773(6)−2.807(8)	2.78(3)	2.49 2.50 2.50[b]	132.6
$[Na(18\text{-}crown\text{-}6)(THF)_2][(C_5Me_5)_2U(SMe)(SCH_2)]$[37]	4	9	2.751(8)−2.813(9)	2.79(2)	2.513 2.535 2.524[b]	132.8
$(C_5Me_5)_2UBr(\eta^2\text{-}{}^tBuNSPh)$[52]	4	9	2.764(13)−2.819(13)	2.80(2)	2.514 2.527 2.521[b]	128.89
$(C_5Me_5)_2UCl[(CH_2)(CH_2)P(Ph)_2]$[58]	4	9	2.75(2) − 2.86(2)	2.80(3)	2.56 2.63 2.60[b]	136.7
	---------	---------				
$[(C_5Me_5)_2U]_2\{[\eta^2\text{-}CO(NMe_2)]\}_2$[59]	4	10	2.72(1)−2.81(1)	2.78(2)	2.502 2.510 2.506[b]	138.0
	---------	---------				
$[(C_5Me_5)_2U(NCMe)_5][BPh_4]_2$[60]	4	11	2.784(4)−2.820(4)	2.80(1)	2.528 2.540 2.534[b]	178.6
$[(C_5Me_5)_2U(NCMe)_5]I_2$[60]	4	11	2.792(11)−2.828(4)	2.81(1)	2.541 2.539 2.540[b]	180.0

[a] Cnt = C_5Me_5 ring centroid. [b] Average. [c] dddt = 5,6-dihydro-1,4-dithiin-2,3-dithiolate. [d] tmed = tetramethylethylenediamine. [e] tpy = terpyridyl.

Table 4. Bond Distances (Å) of Trivalent and Tetravalent Uranium Complexes Containing U−I Bonds from the Cambridge Crystallographic Centre Database Arranged in Order of Increasing U−I Average within Each Oxidation State/Coordination Number Category

complex	oxid. state	coord. no.	U−I distance	U−I avg	U−(μ−I) distance	U−(μ−I) avg
$[UI_2(OPPh_3)_4]I$[61]	3	6	3.157(1) 3.146(1)	3.151(6)		
	---------	---------				
$[U\{\kappa^3\text{-}H(\mu\text{-}H)B(pz^{{}^{t}Bu,Me})_2\}(Hpz^{{}^{t}Bu,Me})I(\mu\text{-}I)]_2$[a,62]	3	7	3.117(2)	3.117(2)	3.215(2)	3.215(2)
$UI_3(THF)_4$[63]	3	7	3.103(2) 3.167(2) 3.119(2)	3.13(3)		
	---------	---------				
$(C_5Me_5)UI_2(THF)_3$[6]	3	8	3.179(1) 3.161(1) 3.162(1) 3.168(1)	3.168(7)		
$(C_5H_4{}^{t}Bu)UI_2(py)_3$[b,64]	3	8	3.1466(11) 3.1912(11)	3.17(2)		
$(tpza)UI_3(THF)$[c,65]			3.1439(6) 3.1914(6) 3.2087(7)	3.183(3)		
$(tpza)UI_3(NCMe)$[c,65]	3	8	3.1632(10) 3.2383(14) 3.2637(10)	3.22(4)		
$UI_3(bipy)_2(py)$[b,d,66]	3	8	3.2032(8) 3.2071(8) 3.2511(8)	3.22(2)		
	---------	---------				
$(C_5H_4{}^{t}Bu)_2UI(py)_2$[64]	3	9		3.174(5)		
	---------	---------				
$IU(OAr)_3$[e,67]	4	4	3.011(2)	3.011(2)		
	---------	---------				
$I_2U(OAr)_2(THF)$[e,67]	4	5	2.982(1) 3.025(1)	3.00(2)		
	---------	---------				
Tp^*UI_3[f,68]	4	6	2.960(1) 2.973(1) 2.969(1)	2.967(5)		
	---------	---------				
$UI_4(py)_3$[b,69]	4	7	2.9857(4) 3.0438(4) 3.0163(4) 2.9558(4)	3.00(3)		
$(SPr^i)_2UI_2(py)_3$[b,70]	4	7		3.093(4)		
$Tp^*UI_3(NCMe)$[f,68]	4	7	2.9980(8) 3.0238(9) 3.3036(7)	3.1(1)		
	---------	---------				
$(C_5Me_5)_3U_3(\mu_3\text{-}I)(\mu_3\text{-}S)(\mu_2\text{-}I)_3I_3$[40]	4	8	2.961(5) 2.943(5) 2.953(5)	2.952(7)	3.240(5) 3.115(5) 3.353(4) 3.068(5) 3.289(5) 3.092(5) 3.094(5) 3.090(5) 3.118(5)	3.16(10)
$[(C_5H_3(SiMe_3)_2]_2UI_2$[71]	4	8	2.953(2) 2.954(2)	2.9535(5)		
$[(C_5Me_5)U(\mu\text{-}I)_2]_3N$[g]	4	8			3.1536(4) 3.1599(4) 3.1623(4) 3.1720(4) 3.1586(4) 3.1617(4) 3.1632(4) 3.2109(4) 3.1483(4) 3.1622(4) 3.1648(4) 3.1825(4)	3.16(2)
$(tpa)U(OMe)I_3$[h,72]	4	8	3.1678(2) 3.1776(2) 3.1931(2)	3.18(1)		
$\{[(tpa)U(\mu\text{-}O)I]_3(\mu_3\text{-}I)\}I_2$[h,72]	4	8	3.2242(5) 3.1861(6) 3.2326(6)	3.21(2)	3.3016(6) 3.2840(6) 3.2754(5)	3.29(1)
$(tpa)U(OMe)_2I_2$[h,72]	4	8	3.1670(3) 3.2634(3)	3.21(4)		
	---------	---------				
$[UI_2(NCMe)_7][UI_6]$[69]	4	9	3.001(2)	3.001(2)		
$(C_5Me_5)_2UI_2(NCPh)$[68]	4	9	2.942(3) 3.092(2)	3.01(8)		

[a] pz = pyrazolyl. [b] py = pyridine. [c] tpza= tris[(2-pyrazinyl)methyl]amine. [d] bipy = bipyridine. [e] OAr = 2,6-di-*tert*-butylphenoxide. [f] Tp* = hydridotris(3,5-dimethylpyrazolylborate). [g] This work. [h] tpa = tris[(2-pyridyl)methyl]amine.

coordinate U^{4+} hydride could not be differentiated from an *n*-coordinate U^{3+} complex on the basis of $U-C(C_5Me_5)$ distances.[28]

Similarly, there is no particular range of (C_5Me_5 ring centroid)$-U-$(C_5Me_5 ring centroid) angles for trivalent and tetravalent metallocenes. The 5 eight-coordinate U^{3+} structures have a 127.9−135.7° range compared to 126.2−142.6° for the 15 eight-coordinate U^{4+} structures and 128.4−136.7° for the 12 nine-coordinate U^{4+} structures.

In addition to these analyses of $U-C(C_5Me_5)$ distances, U−I bond distances were surveyed in 23 U^{+3} and U^{4+} compounds in the Cambridge Crystallographic Data Centre database. The distances are compiled in Table 4. Only three involved bridging iodides. The single U^{3+} example had an average U−(*μ*-I) of 3.215(2) Å that was in the middle of the 3.16(10) and 3.29(1) Å averages of the U^{4+} examples. The 3.153(4)−3.2109(4) Å range in **2** overlaps the U^{4+} and U^{3+} averages. The average U−I terminal distances for 9 U^{3+} complexes range from 3.13(3)−3.22(2) Å compared to a range of 2.952(7)−3.21(2) Å for 14 U^{4+} complexes. This shows that there is considerable overlap in the U−I distances in both U^{3+} and U^{4+} iodide complexes and that no particular trend is observed in these data either.

APCI-MS. To resolve the problem of identifying the central atom E in $[(C_5Me_5)U(\mu\text{-}I)_2]_3E$, it was desirable to obtain mass spectrometric data on **2** and an analogue made from ^{15}N-substituted azide, $Na^{15}NNN$. Because ^{15}N azide is substituted with ^{15}N on only one of the terminal ends, the azide to nitride conversion in eq 5 could put 50% ^{15}N into

$$2\,^{15}\mathrm{N}{=}\mathrm{N}{=}\mathrm{N}^{1-} + 4\mathrm{e}^- \rightarrow \mathrm{N}^{3-} + {}^{15}\mathrm{N}^{3-} + \mathrm{N}_2 + {}^{15}\mathrm{NN} \tag{5}$$

a nitride product arising from azide assuming the conventional mechanism for azide to nitride conversion. Mass spectrometry would be ideal for determining ^{15}N incorporation in this paramagnetic complex.

Attempts to obtain mass spectrometric data on **2** using electrospray mass spectrometry (ESMS), a technique that had previously been successful with a variety of organolanthanide complexes,[29] were unsuccessful. The conditions of the ESMS technique can encourage redox chemistry that can degrade the analytes. APCI-MS was attractive because it does not run the risk of this type of electrochemical degradation. Previously, APCI-MS had been considered primarily as a methodology for analyzing organic compounds of molecular weights up to 1000 amu.

APCI-MS conditions typically involve a flow rate of 0.2−1.0 mL min^{-1}, a temperature of 500 °C, and a corona discharge current of 5 *μ*A. Variation of these conditions revealed that, for **1** and **2**, a lower flow rate (50 *μ*L min^{-1}), temperature (250 °C), and corona discharge current (1 *μ*A) gave a better signal. It should be noted, however, that some current was required. No ions were seen if the current was switched off, a condition that is akin to thermospray, an

---

(28) Evans, W. J.; Miller, K. A.; Kozimor, S. A.; Ziller, J. W.; DiPasquale, A. G.; Rheingold, A. L. *Organometallics* **2007**, *26*, 3568.

(29) Evans, W. J.; Johnston, M. A.; Fujimoto, C. H.; Greaves, J. *Organometallics* **2000**, *19*, 4258.

(30) Evans, W. J.; Kozimor, S. A.; Ziller, J. W. *Polyhedron* **2004**, *23*, 2689.

(31) Evans, W. J.; Kozimor, S. A.; Ziller, J. W.; Kaltsoyannis, N. *J. Am. Chem. Soc.* **2004**, *126*, 14533.

(32) Evans, W. J.; Nyce, W. G.; Forrestal, K. J.; Ziller, J. W. *Organometallics* **2002**, *21*, 1050.

(33) Boisson, C.; Berthet, J.-C.; Ephritikhine, M.; Lance, M.; Nierlich, M. *J. Organomet. Chem.* **1997**, *533*, 7.

(34) Manriquez, J. M.; Fagan, P. J.; Marks, T. J.; Vollmer, S. H.; Day, V. W. *J. Am. Chem. Soc.* **1979**, *101*, 5075.

(35) Roger, M.; Belkhiri, L.; Thuéry, P.; Arliguie, T.; Fourmigué, M.; Boucekkine, A.; Ephritikhine, M. *Organometallics* **2005**, *24*, 4940.

(36) Mehdoui, T.; Berthet, J.-C.; Thuéry, P.; Ephritikhine, M. *Chem. Commun.* **2005**, 2860.

(37) Arliguie, T.; Lescop, C.; Ventelon, L.; Leverd, P. C.; Thuéry, P.; Nierlich, M.; Ephritikhine, M. *Organometallics* **2001**, *20*, 3698.

(38) Arney, D. S. J.; Burns, C. J. *J. Am. Chem. Soc.* **1995**, *117*, 9448.

(39) Evans, W. J.; Kozimor, S. A.; Ziller, J. W. *Organometallics* **2005**, *24*, 3407.

(40) Clark, D. L.; Gordon, J. C.; Huffman, J. C.; Watkin, J. C.; Zwick, B. D. *New J. Chem.* **1995**, *19*, 495.

(41) Barnea, E.; Andrea, T.; Kapon, M.; Berthet, J.-C.; Ephritikhine, M.; Eisen, M. S. *J. Am. Chem. Soc.* **2004**, *126*, 10860.

(42) Lescop, C.; Arliguie, T.; Lance, M.; Nierlich, M.; Ephritikhine, M. *J. Organomet. Chem.* **1999**, *580*, 137.

(43) Gradoz, P.; Baudry, D.; Ephritikhine, M.; Lance, M.; Nierlich, M.; Vigner, J. *J. Organomet. Chem.* **1994**, *466*, 107.

(44) Duttera, M. R.; Day, V. W.; Marks, T. J. *J. Am. Chem. Soc.* **1984**, *106*, 2907.

(45) Evans, W. J.; Kozimor, S. A.; Ziller, J. W. *Chem. Commun.* **2005**, 4681.

(46) Kiplinger, J. L.; Morris, D. E.; Scott, B. L.; Burns, C. J. *Organometallics* **2002**, *21*, 3073.

(47) Schelter, E. J.; Veauthier, J. M.; Thompson, J. D.; Scott, B. L.; John, K. D.; Morris, D. E.; Kiplinger, J. L. *J. Am. Chem. Soc.* **2006**, *128*, 2198.

(48) Straub, T.; Frank, W.; Reiss, G. J.; Eisen, M. S. *J. Chem. Soc., Dalton Trans.* **1996**, 2541.

(49) Arney, D. S. J.; Schnabel, R. C.; Scott, B. L.; Burns, C. J. *J. Am. Chem. Soc.* **1996**, *118*, 6780.

(50) Ventelon, L.; Lescop, C.; Arliguie, T.; Leverd, P. C.; Lance, M.; Nierlich, M.; Ephritikhine, M. *Chem. Commun.* **1999**, 659.

(51) Enriquez, A. E.; Scott, B. L.; Neu, M. P. *Inorg. Chem.* **2005**, *44*, 7403.

(52) Danopoulos, A. A.; Hankin, D. M.; Cafferkey, S. M.; Hursthouse, M. B. *J. Chem. Soc., Dalton Trans.* **2000**, 1613.

(53) Pool, J. A.; Scott, B. L.; Kiplinger, J. L. *J. Am. Chem. Soc.* **2005**, *127*, 1338.

(54) Boisson, C.; Berthet, J.-C.; Lance, M.; Nierlich, M.; Ephritikhine, M. *J. Organomet. Chem.* **1997**, *548*, 9.

(55) Cramer, R. E.; Roth, S.; Gilje, J. W. *Organometallics* **1989**, *8*, 2327.

(56) Cramer, R. E.; Ariyaratne, K. A. N. S.; Gilje, J. W. *Z. Anorg. Allg. Chem.* **1995**, *621*, 1856.

(57) Ariyaratne, K. A. N. S.; Cramer, R. E.; Jameson, G. B.; Gilje, J. W. *J. Organomet. Chem.* **2004**, *689*, 2029.

(58) Cramer, R. E.; Roth, S.; Edelmann, F.; Bruck, M. A.; Cohn, K. C.; Gilje, J. W. *Organometallics* **1989**, *8*, 1192.

(59) Fagan, P. J.; Manriquez, J. M.; Vollmer, S. H.; Day, C. S.; Day, V. W.; Marks, T. J. *J. Am. Chem. Soc.* **1981**, *103*, 2206.

(60) Mayandié, J.; Berthet, J.-C.; Thuéry, P.; Ephritikhine, M. *J. Am. Chem. Soc.* **2006**, *128*, 1082.

(61) Berthet, J.-C.; Nierlich, M.; Ephritikhine, M. *Polyhedron* **2003**, *22*, 3475.

(62) Maria, L.; Domingos, Á.; Santos, I. *Inorg. Chem.* **2003**, *42*, 3323.

(63) Clark, D. L.; Sattelberger, A. P.; Bott, S. G.; Vrtis, R. N. *Inorg. Chem.* **1989**, *28*, 1771.

(64) Mehdoui, T.; Berthet, J.-C.; Thuéry, P.; Ephritikhine, M. *Dalton Trans.* **2005**, 1263.

(65) Mazzanti, M.; Wietzke, R.; Pécaut, J.; Latour, J.-M.; Maldivi, P.; Remy, M. *Inorg. Chem.* **2002**, *41*, 2389.

(66) Riviére, C.; Nierlich, M.; Ephritikhine, M.; Madic, C. *Inorg. Chem.* **2001**, *40*, 4428.

(67) Avens, L. R.; Barnhart, D. M.; Burns, C. J.; McKee, S. D.; Smith, W. H. *Inorg. Chem.* **1994**, *33*, 4245.

(68) Enriquez, A. E.; Scott, B. L.; Neu, M. P. *Inorg. Chem.* **2005**, *44*, 7403.

(69) Berthet, J.-C.; Thuéry, P.; Ephritikhine, M. *Inorg. Chem.* **2005**, *44*, 1142.

(70) Leverd, P. C.; Lance, M.; Vigner, J.; Nierlich, M.; Ephritikhine, M. *Dalton Trans.* **1995**, 237.

(71) Blake, P. C.; Lappert, M. F.; Taylor, R. G.; Atwood, J. L.; Hunter, W. E.; Zhang, H. *Dalton Trans.* **1995**, 3335.

(72) Karmazin, L.; Mazzanti, M.; Pécaut, J. *Inorg. Chem.* **2003**, *42*, 5900.

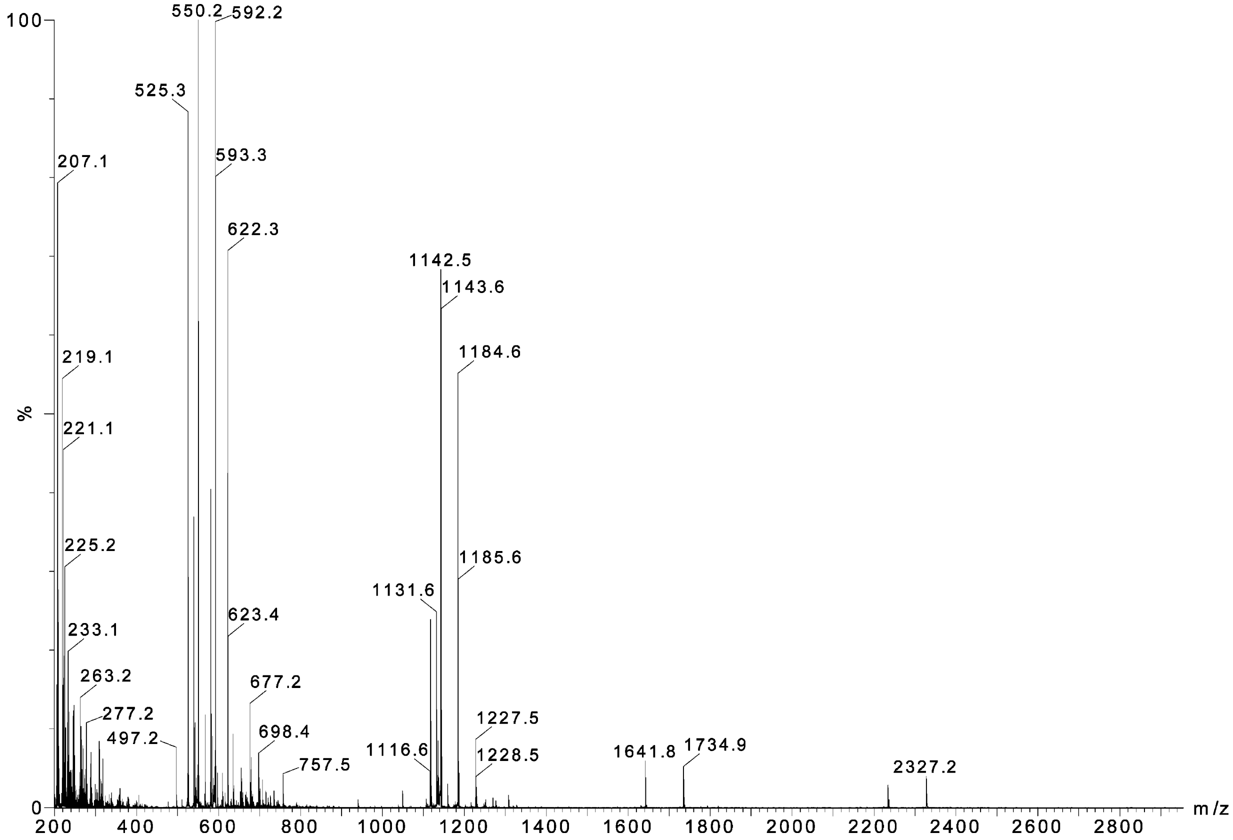

Figure 3. APCI-MS spectrum of **1**.

earlier method of ionizing samples in liquid matrices, but without the ammonium salt used in that technique. The corona discharge acts in place of the filament used in conventional chemical ionization. The discharge initially ionizes the solvent molecules, which are present in great excess. Ion/molecule reactions within the solvent yield protonated solvent molecules that can potentially act as charge- and proton-transfer reagents to ionize the analyte of interest.

Trimeric **1** did not produce a signal in the molecular ion region but provided very obvious fragments of $[M - N_3]^+$ and $[M - C_5Me_5]^+$ at $m/z = 1734$ and 1641, respectively (Figure 3). Primary ions in the rest of the spectrum included bimetallic and monometallic fragments such as $[(C_5Me_5)_4(N_3)_3U_2]^+$ and $[(C_5Me_5)_4(N_3)_4U_2]^+$ at $m/z = 1142$ and 1184 and $[(C_5Me_5)_2N_3U]^+$ and $[(C_5Me_5)_2(N_3)_2U]^+$ at $m/z = 550$ and 592, respectively. Interestingly, there were also ions at $m/z = 2327$ and 2234 corresponding to $\{[(C_5Me_5)_2U(N_3)_2]_4 - N_3\}^+$ and $\{[(C_5Me_5)_2U(N_3)_2]_4 - C_5Me_5\}^+$, suggesting that **1** may be capable of different degrees of oligomerization than the trimeric form seen in the crystalline state.

The molecular ion region of mass spectra generated for **2** synthesized with ^{14}N showed $m/z = 1894.9$ and 1895.9. These peaks are consistent with $[M]^+$ and a protonated molecule, $[M + H]$, respectively, arising from a combination of charge- and proton-transfer ionizations where $M = [(C_5Me_5)U(\mu\text{-}I)_2]_3N$ (Figure 4). The ratio of these ions was dependent on the temperature of the APCI-MS probe. Lower temperature operation at 250 °C increased the $[M + H]^+$ ion, although this ion was still only present at approximately 65% of the $[M]^+$ intensity (Figure 5). The ratio of these peaks and the next higher mass peak due to ^{13}C incorporation was 100:100:18 for $[M]^+/[^{13}CM]^+$ and $[M + H]^+/[^{13}CM + H]^+$ and $[^{13}C_2M]^+$, respectively.

If $[(C_5Me_5)U(\mu\text{-}I)_2]_3O$ were present, this would be expected to increase the $m/z = 1896.9$ ion. In addition, "$\{[(C_5Me_5)U(\mu\text{-}I)_2]_3O\}^{+}$" ions incorporating ^{13}C should give larger intensities at $m/z = 1897$ and 1898 than were observed. Calculations to evaluate this point more quantitatively were made on the 250 °C spectrum of **2** in which the $m/z = 1894.9$ peak was observed at 99% intensity for ions in the molecular ion region. Assuming this peak arises from $\{[(C_5Me_5)U(\mu\text{-}I)_2]_3N\}^+ = [M]^+$, the $m/z = 1895.9$ peak would be expected to have a 34% relative intensity arising from an $[M]^+$ containing one ^{13}C atom. Because the $m/z = 1895.9$ peak has an intensity of 100% relative to the $m/z = 1894.9$ peak, it appears that 66% of $m/z = 1895.9$ arises from $[M + H]^+$. The peak at $m/z = 1896.9$ should have contributions from $[M]^+$ with two ^{13}C atoms (5.6% intensity relative to the $m/z = 1894.9$ peak) and from $[M + H]^+$ with one ^{13}C atom (22% relative intensity). The total of these intensities, 27.6%, is equivalent to all of the intensity observed at $m/z = 1896.9$, which was 24.4%. Because the observed intensity for $m/z = 1896.9$ can be entirely accounted for by nitride-containing ions, i.e., $\{[(C_5Me_5)U(\mu\text{-}I)_2]_3N\}^+$ with two ^{13}C atoms and $\{[(C_5Me_5)U(\mu\text{-}I)_2]_3N + H\}^+$ with one ^{13}C atom, this suggests that there is very little, if any, $[(C_5Me_5)U(\mu\text{-}I)_2]_3O$ in the sample. A similar result was found with a spectrum taken at 500 °C. In this case, the intensities were 100% $[M]^+$, 52% $[M + 1]^+$, and 10% $[M + 2]^+$ (again based on intensities in

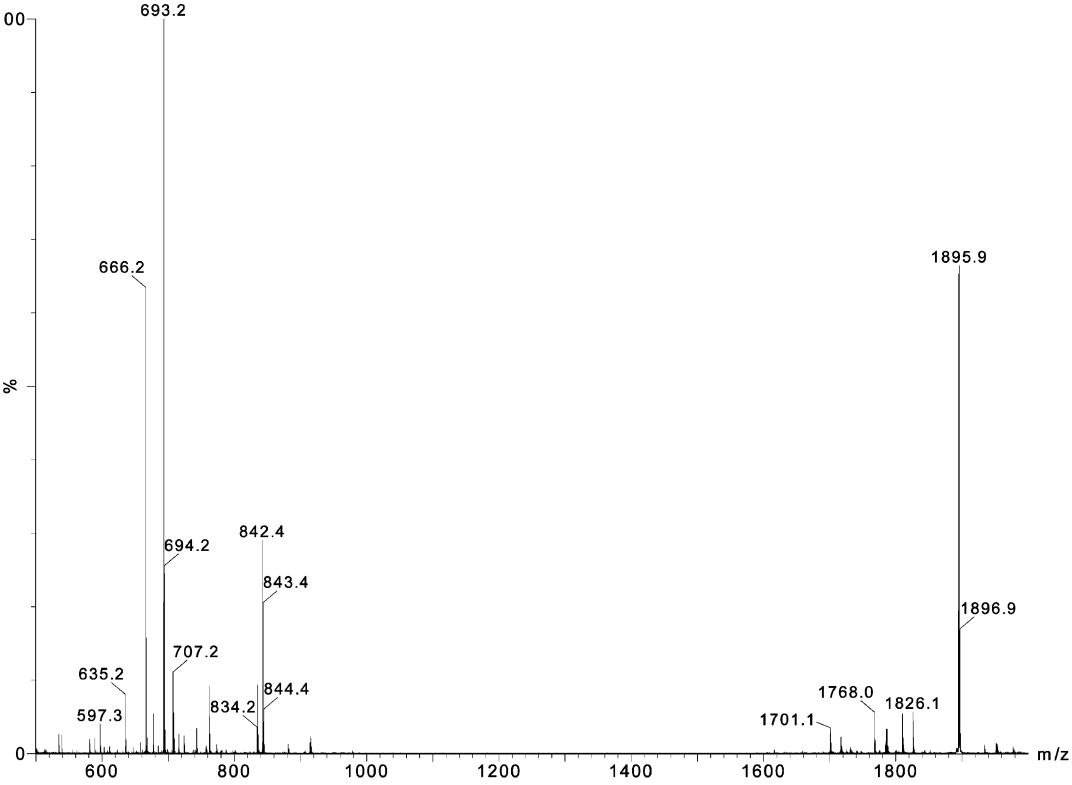

Figure 4. APCI-MS spectrum of **2** at 250 °C.

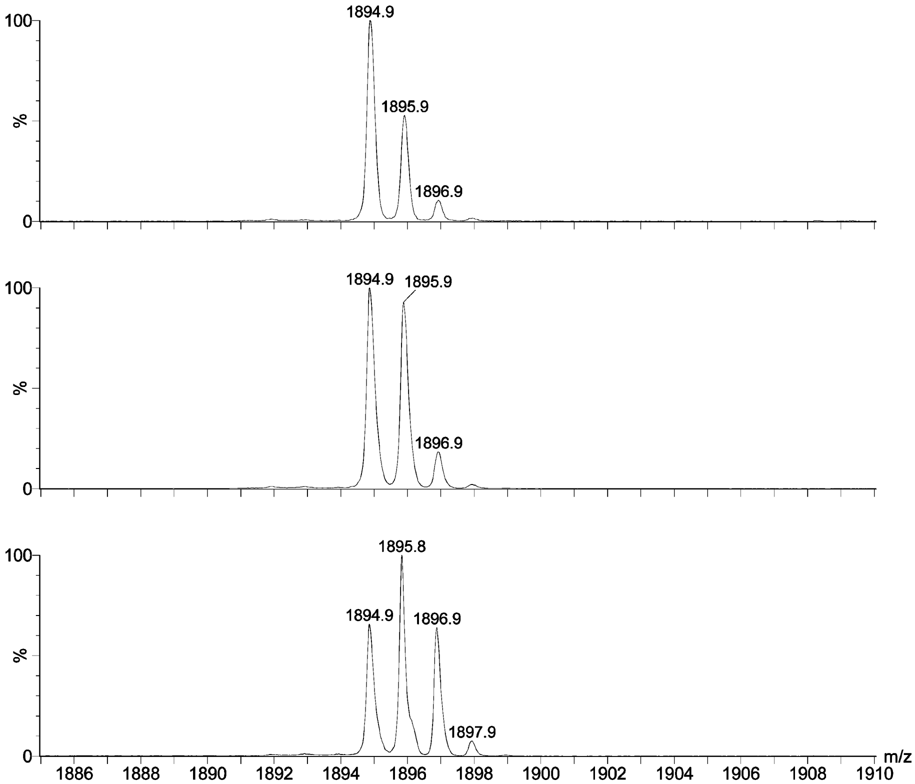

Figure 5. APCI-MS spectra of **2** at 500 °C (top) and at 250 °C (middle) and 50% ^{15}N-labeled **2** at 250 °C (bottom).

the molecular ion region). The sum of the intensities of a nitride-containing $[M]^+$ ion containing two ^{13}C atoms (5.7%) and a $[M + H]^+$ ion containing one ^{13}C atom (6%) was again slightly larger than the 10% intensity observed for the *m*/*z* = 1896.9 ion at which $\{[(C_5Me_5)U(\mu\text{-}I)_2]_3O\}^+$ would be observed.

Calculations were also done on the exact mass expected for the *m*/*z* = 1896.9 peak in the 250 °C spectrum. The exact mass calculated for a sample containing the mixture of nitride-containing $[M]^+$ and $[M + H]^+$ given above should be *m*/*z* = 1896.9445. The observed mass was *m*/*z* = 1896.9457. In comparison, 5% incorporation of an oxide would give a calculated mass of $m/z = 1896.9406$ and 10% oxide would give $m/z = 1896.9366$. Hence, the observed peak is much closer to the nitride-containing exact mass than to the masses likely if oxide were present. In summary, neither isotope ratios nor exact masses show any evidence for oxide-containing impurities.

When compound **2** was synthesized with Na^{15}NNN, with the single label at one end of the three-nitrogen chain, the incorporation of N/^{15}N at 1:1 would be expected to give a 50:100:55:5 ratio in the molecular ion region, where 50 corresponds to $[M]^+$. This is close to the 65:100:65:5 ratio that was observed. Figure 5 shows the molecular ion regions for the NaNNN and Na^{15}NNN reaction products. The change in the relative intensities with the ^{15}N-labeled azide precursor is consistent with the presence of a nitride rather than an oxide. The similarity of observed intensities to those calculated for 50% incorporation is consistent with the assumption of nitride incorporation according to eq 5.

Discussion

The results obtained show that the APCI-MS technique is an effective mass spectrometric option for analyzing air- and moisture-sensitive organometallic f element complexes. Although a parent ion was not observed for **1**, significant fragment ions as well as ions suggestive of higher degrees of oligomerization were found. For **2**, fragment ions as well as a parent ion were obtained, and these allowed the identification of the central ion as nitrogen, a determination not possible by X-ray crystallography.

The APCI-MS results for **2** clearly demonstrate that the atom contained within the U_3 triangle is nitrogen. The molecular weight is 2 amu less than would be seen for oxygen and 3 amu less than that for hydroxide. In addition, the isotope pattern fits the expected pattern for the inclusion of ^{15}N from Na^{15}NNN. The presence of oxygen or hydroxide as a central atom would provide a very different isotope pattern in the molecular ion region as well as a change of the molecular weight.

The identification of **2** as a nitride indicates that azide to nitride conversions are not limited to the $[(C_5Me_4R)_2U][(\mu\text{-}Ph)_2BPh_2]/NaN_3$ (R = Me, H) reactions that formed $[(C_5Me_4R)_2U(\mu\text{-}N)(C_5Me_5)_2U(\mu\text{-}N_3)]_4$. This type of reaction can also occur with trivalent $(C_5Me_5)UI_2(THF)_3$. In the $[(C_5Me_4R)U][(\mu\text{-}Ph)_2BPh_2]/NaN_3$ reactions, likely intermediates were $(C_5Me_4R)_2UN_3$. In the case of **2**, it was expected that metathesis with iodides could provide azide complexes such as "$(C_5Me_5)UI(N_3)(THF)_x$". Because the iodide to uranium ratio in the starting material is retained in the product, this reaction must be more complicated than a simple ionic metathesis followed by reduction of azide. This may account for the low yield of the product.

A comparison of U−C(C$_5$Me$_5$), U−(C$_5$Me$_5$ ring centroid), and U−I distances in the U^{3+} and U^{4+} complexes in the literature shows that the ranges overlap considerably. The typical 0.1 Å demarcation found between Ln^{2+} and Ln^{3+} metallocene complexes is not found for these uranium complexes. Although U^{3+} complexes tend to have slightly larger bond distances compared to U^{4+}, the difference is not large enough to make this a definitive means of analyzing the oxidation state. The regularity of the lanthanides compared to the actinides and to transition metals is consistent with the fact that the lanthanides are the most ionic of these three classes of complexes.

Conclusion

APCI-MS has proven to be viable with air-sensitive organoactinide complexes. With $[(C_5Me_5)U(\mu\text{-}I)_2]_3N$, this provided essential isotopic identification of the central atom as nitride and provided another example of a U^{3+}-induced azide to nitride conversion. Analysis of U−C(C$_5$Me$_5$) and U−I metrical parameters in U^{3+} and U^{4+} metallocene complexes shows that there is considerable overlap between the U−C and U−I distances in the two classes of complexes.

Acknowledgment. We thank the Chemical Sciences, Geosciences, and Biosciences Division of the Office of Basic Energy Sciences of the Department of Energy for support.

Supporting Information Available: X-ray diffraction details (CIF) and X-ray data collection, structure, solution, and refinement of compounds **1** and **2** (PDF). This material is available free of charge via the Internet at http://pubs.acs.org.

IC7006099